INTELLIGENT HEALTH MONITORING AND DAMAGE IDENTIFICATION OF A COMPOSITE ANTENNA SUB-REFLECTOR

A. Panopoulou[1], D. Roulias[1], T. Loutas[1], V.Kostopoulos[1*] , V.J. Gómez Molinero[2]

[1] *Applied Mechanics Laboratory, Mechanical Engineering & Aeronautics Department, University of Patras, GR-26500 Rio-Patras, Achaia, Greece*
[2] *EADS CASA Espacio, Avenida de Aragon 404, E-28922 Madrid, Spain*
**kostopoulos@mech.upatras.gr*

Keywords: wavelet, fiber bragg gratings, structural health monitoring

Abstract
This paper presents a structural health monitoring system for composite aerospace structures based on wavelet feature extraction and artificial neural network (ANN). The system is developed and tested on a composite antenna sub-reflector, manufactured by EADS Casa Espacio. Real damage is induced to the structure by means of crack on the CFRP skin. The crack is initially the minimum detectable, according to the finite element analysis, and as a second step, is increased in order multiple crack sizes to be obtained at the same point. Optical sensors, specifically Fiber Bragg Grating (FBG) sensors, are mounted in an optimum topology on the sub-reflector in order to monitor the responses at different vibration levels. Wavelet-based techniques consist the base for feature extraction of the dynamic signals. Discrete wavelet transform (DWT) is used among other tools for the signal processing scheme. The extracted features consist the input for the Artificial Neural Network scheme which was applied as classification tool. ANNs have emerged as a powerful technique for general purpose pattern recognition. ANNs were used to create an intelligent expert system able to distinguish between different damage states. Potential applications of the proposed structural health monitoring system is for acceptance and qualification of manufactured components, for ground qualification tests and for support maintenance and, in long term, during the mission for continuous spacecraft monitoring.

1 Introduction

A fundamental issue in aerospace industry concerns continuous monitoring of the structural condition for damage detection and identification. Many techniques have emerged over the last years with the attention focused on smart structures with inherent sensing capabilities. To this direction dynamic strain measurements using Fiber Bragg Grating (FBG) sensors for vibration-based structural health monitoring is a quite promising technique [1], especially in composite structures, where the FBGs can be integrated into the material or fixed as patches on the surface. Fiber Bragg Grating technology offers many advantages, improving in various ways the already sensing systems and enabling new monitoring applications that were not possible by using conventional sensing technologies [2]. In few recent works, FBG's have been utilized for modal analysis and damage detection. In [3] Mieloszyk et al. demonstrated

an adaptive wing for small aircraft applications with an array of FBGs for evaluation of the wing condition. Dragan et al. [4] used FBGs on specimens made from helicopter blades to characterize possibility of SHM application in main rotor blade of military helicopters. In [5] Dvorak et al. embedded FBGs into the adhesive layer of skin specimens to detect disbonding under fatigue tests. In [6] Guemes et. al. demonstrated that FBGs can detect damage by measuring sudden changes in the strain distribution of composite structures due to delaminations or debonding of stiffening elements. Lee et. al. [7] used Fiber Bragg Gratings to measure dynamic strains inside a subscale wing under real-time wind tunnel testing. He also used electric strain gauge and PZT sensor as reference. The agreement among the three sensors was confirmed in bench test. Chambers et. al. [8] assessed the ability of FBGs embedded in a composite laminate to detect damage caused by a low velocity impact. The results from the optical sensors indicated that there was an increasing resultant strain with increasing impact energy. This conclusion was in agreement with the results from the acoustic emission testing. Finally, EADS Airbus used FBGs mounted on the surface of a composite wing structure to monitor strain during loading and with change of temperature [9].

In this work, the development of the structural health monitoring system based on FBGs and dynamic measurements was implemented. The whole system was validated on a real structure, an antenna sub-reflector, tested in EADS CASA ESPACIO under vibration testing. Damage was initially simulated by means of added masses on different positions on the sub-reflector. Real damage was also introduced to the structure by means of interface bolts' removal and of cracks on the skin. FBG sensors were successfully utilized for dynamic strain measurements and the results are in agreement with the FEA results for all damage scenarios. Concerning the damage detection expert system, statistical features were used, including DWT, and ANN techniques. The system showed high reliability, confirmed by the ability of the ANN to recognize the presence of all damages and their position on the real aerospace hardware.

2 Feature extraction and expert system development

Feature extraction is essential in data analysis in order to enhance damage identification. A feature is any parameter of the measured response that is extracted through signal processing. In feature extraction "data" are transformed into "information" [10]. The final objective is to find features sensitive to damage and insensitive to noise-induced situations. Changes of features are an indication of damage. Generally, the choice of features is based on a trade-off between the computational feasibility related to low-level features and extensive preprocessing required for high-level features [11]. Detailed information about feature extraction can be found in [12] [13]. The main advantage of feature extraction that ideally the features are more stable and well behaved than the raw data. In addition, the features provide a reduced data set for the scheme of pattern recognition. Figure 1 summarizes the overall intelligent chain of processing for a multi-sensor architecture.

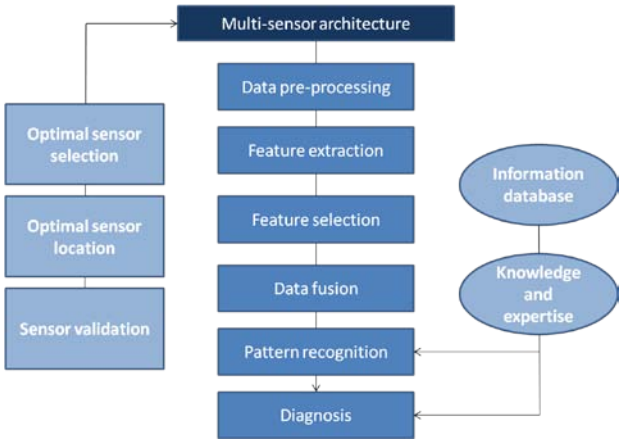

Figure 1. Signal processing for a multi-sensor architecture

In this work, the vectors from the sensors located closer to the interfaces (high strain), were kept as features. The indices derived from the wavelet transform algorithm together with the time domain indices (skewness, kurtosis, standard deviation) and the frequency domain indices (derived from the Power Spectra Density via Welch method) comprised the input for the Artificial Neural Network for each damage case. Each feature is normalized to [-1,1] in order to be fed into the artificial neural network scheme. All calculations were implemented with the Matlab® Wavelet Toolbox.

3 FEM and Vibration Testing

The antenna sub-reflector is equipped with three blades that support the dish. The diameter of the sub-reflector is equal to 0.9m, the thickness is 16.62 mm and the total mass is equal to 1.5 kg. The thickness of the CFRP top and bottom face is 0.31mm. The finite element model was generated by utilizing MSC PATRAN pre and postprocessor. The dish is modeled with shell elements (QUAD) and is divided in seven parts with different core orientation. The eigenvalue analysis results were obtained by the MSC NASTRAN code with the reflector constrained at the support structure interface. Normal modes were calculated using MSC NASTRAN SOL 103. Figure 2 illustrates the strain mode shapes for the first 3 modes. By calculating the strain in different elements, it was decided whether the sensors are going to be put in tangential or circumferential direction. In the majority of the eigenmodes, the strain has higher values in the tangential direction. For that reason, more strain sensors have to be mounted in this direction and less in the circumferential. The optimum sensor topology, which includes 40 FBGs, is presented in Figure 3. In total, 32 FBGs are placed in the tangential direction and 8 FBGs in the circumferential.

The installation tools include the Strain Gauge Installation Kit, a UV radiation source (Omnicure® 1000) and the optical strain gauges. High strength coated FBG sensors (SG-01 FOS&S®, coating ORMOCER, FC/APC connector), 40 in total, positioned in a serial configuration in two different optical fibers, were used for conducting the experiments (Draw Tower Grating Chain). The structural dynamic behavior has been numerically simulated and experimentally verified by means of vibration testing.

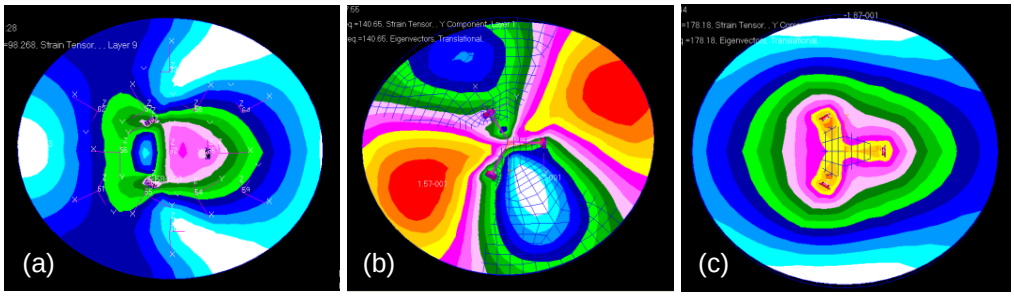

Figure 2. Analytical mode shapes based on strain of the antenna sub-reflector for the 1st(a), 2nd(b) and 3rd (c) natural frequencies

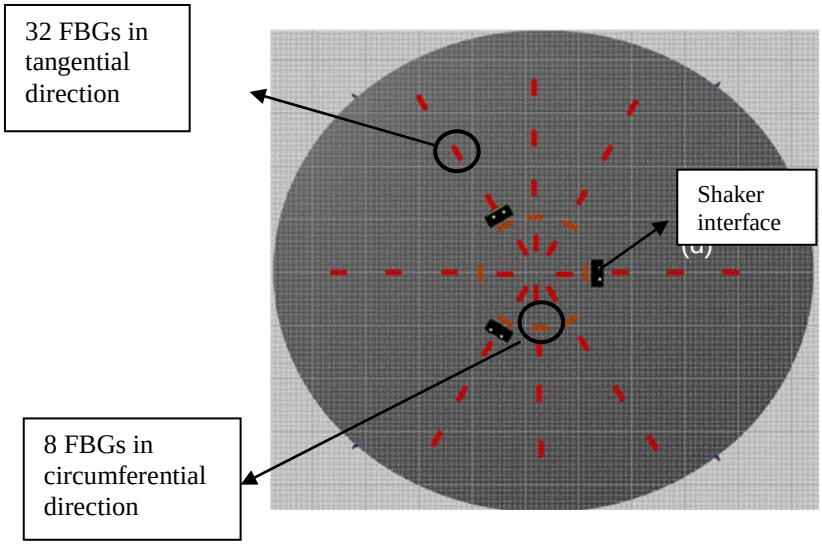

Figure 3: Sensor topology on the antenna sub-reflector

The sub-reflector was mounted on the 489N electrodynamic shaker via the 3 blades. The torque of the bolts between the blades of the sub-reflector and the interface plate, as well as between the interface plate and the shaker, were measured and controlled with a torque meter. The vibrator has been employed to excite the structure with sine sweep excitation in the frequency range of interest (20-500Hz) at 2g level (2 octaves / minute). Tests under 0.5g, 1g also were conducted often in order to verify the experimental setup. Initially, series of tests on the pristine structure took place and the agreement between the Fiber Bragg Gratings results and those of the accelerometer was verified.

The tests were initiated on the structure without any damage and several repetitions were conducted. As a second step, the structure was divided, into four areas. At each area damage was simulated by adding different lumped masses (27grams, 49 grams), in order to obtain data for different damage sizes and locations. The mass was located within a zone ±3cm from the centre of each area (areas 1-4, Table 1). Repetitions were conducted for each damage state. The experimental process continued by provoking real damage to the structure. In the first real damage case scenario, the bolt of the blade (one bolt each time) was removed (in two different blades in total, A and B, Table 1). These blades connect the sub-reflector with the interface plate and the shaker. Several test runs were conducted for both damage states. At the second real damage scenario, a minimum detectable crack (according to FEM) was provoked

on the CFRP skin, close to one of the interfaces (close to point A, Table 1). The initial crack size was equal to 15mm. After conducting several repetitions of the above damage state, multiple cracks of different sizes were provoked at the same location. The crack was increased to 38mm, 68mm and finally to 100mm. Table 1 summarizes all the damage cases (simulated and real damage cases).

	DAMAGE CASE	**SIZE**	**LOCATION**
0	Pristine state	-	-
1	Added mass	27 gr	1
2	Added mass	27 gr	2
3	Added mass	27 gr	3
4	Added mass	27 gr	4
5	Added mass	49 gr	1
6	Added mass	49 gr	2
7	Added mass	49 gr	3
8	Added mass	49 gr	4
9	Remove bolt	-	A
10	Remove bolt	-	B
11	Crack 1 (on the skin)	15 mm	Close to A
12	Crack 2 (on the skin)	38 mm	
13	Crack 3 (on the skin)	68 mm	
14	Crack 4 (on the skin)	100 mm	

Table 1: Damage cases

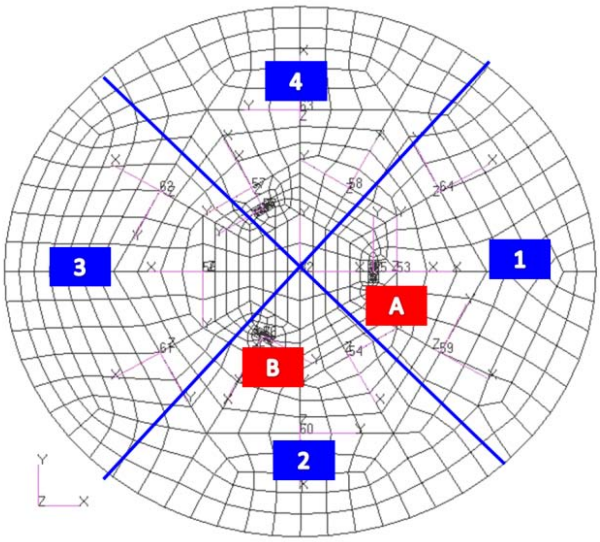

5 Results

The fiber optic sensors measured frequencies up to 500 Hz and all eigen frequencies were compared successfully with the results of the accelerometer and of the analytical model. Indicatively, Table 2 illustrates the first 4 eigen-frequencies of the sub-reflector in the healthy state, without bolt and with minimum crack, measured by the FBGs, the accelerometer and calculated by the FEM. All damage states were simulated in the analytical model.

No damage	MODE 1	MODE 2	MODE 3	MODE 4

FBG	98.5	142	182	301
ACCELEROMETER	98.6	142	182	302
FEM	98.3	141	178	299

(a)

Bolt removed	MODE 1	MODE 2	MODE 3	MODE 4
FBG	97.6	141	182	300
ACCELEROMETER	97.5	142	181	301
FEM	98	141	178	299

(b)

Minimum crack (crack 1)	MODE 1	MODE 2	MODE 3	MODE 4
FBG	98	140.5	181	300
ACCELEROMETER	97.5	142	182	302
FEM	97.5	141	178	298

(c)

Table 2: Eigen frequencies of the sub-reflector without any damage (a), without bolt (b), with minimum crack (c)

After the waveforms are acquired they are evaluated. At first, a visual inspection of the waveforms along with the corresponding spectrum takes place (Figure 4a, 4b). It is evident that the waveforms are corrupted by noise. This noise can be attributed to round off error oscillations (the structure response is close to the limit of the sensor dynamic range) and possible contextual noise. In order to enhance the geometric and physical characteristics of the signal, a simple wavelet shrinkage scheme is applied. The configuration of this scheme is as follows

- Wavelet denoising scheme: according to [14]
- Wavelet type: db4
- Levels of decomposition: 4
- Threshold type: hard threshold
- Threshold value: threshold defined by neighcoefs method [14]

The results are depicted in Figure 4c, 4d. The round off oscillations are disposed from the time domain signal. Moreover, the frequency content of the signal is improved. The DC component is disposed as well as false spectral peaks (70 Hz peak at Figure 4d). Moreover, few modal peaks are uncovered (Figure 4d in the vicinity of 300 Hz).

Based on the results derived from each sensor, statistical features extracted from the time domain, frequency domain and the combined time-frequency domain via the Discrete Wavelet Transform have been used to monitor non-destructively any change in structural integrity of the sub-reflector, due to the introduction of the damage**.**

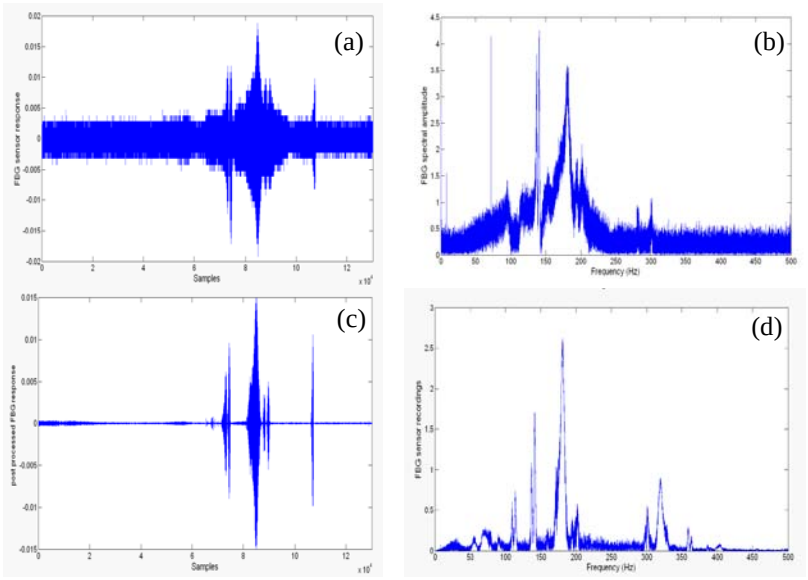

Figure 4: An original FBG sensor recording derived from sensor positioned in the centre of area 2 and its corresponding spectrum (a,b). The post denoising time domain signal and its corresponding spectrum (c,d)

These features are the input for the ANN scheme. The ANN in the current study comprises a feed forward multilayer perceptron with input (number of neurons is equal to the number of input indices according to each damage case), one hidden layer with 11, 8 and 12 neurons for the added masses, bolt removal and crack scenario respectively, and one output layer (number of neurons is equal to the number of outputs based on each damage case). The transfer function depends on the classification scheme. Since, in our case, the mapping is to [-1,1] for each output, the standard hyperbolic tangent of the weighted sum was utilized. The optimization criterion that was utilized was the sum of square errors. The standard Levenberg–Marquardt backpropagation algorithm was utilized to train the ANN model. The whole neural network scheme was implemented with the Matlab® Neural Network Toolbox. Due to the stochastisity, multiple training efforts of each ANN model were necessary in order to obtain a trustworthy efficiency measure. The classification efficiency (%) for all damage scenarios were calculated for the case of lumped masses (9 damage states) equal to 88%, for the case of the removed bolt (3 damage states) equal to 89% and for the case of the four different cracks on the skin (5 damage states) the classification efficiency was equal to 86% (Table 2).

	Damage cases		
	ADDED MASSES	**NO I/F BOLT**	**CRACK**
Number of hidden neurons	11	8	12
ANN optimization algorithm	Levenberg Marquadt		
Training examples	261	36	90

Testing examples	129	18	30
Correct mappings / Total Test mappings * 100%	88%	89%	86%

Table 2: ANN classification results for the antenna sub-reflector

REFERENCES

[1] Staszewski, W., Boller, C., Tomlinson, G. *Health Monitoring of Aerospace Structures: Smart sensor technology and signal processing*. John Wiley & Sons Inc., England, (2004).
[2] Dunphy, J.R., Meltz, G., Morey, W.W. Optical Fiber Bragg Grating Sensors: A candidate for Smart Structures Application. In Udd, E., ed., *Fiber Optic Smart Structures*. John Wiley & Sons Inc., NY, (1995).
[3] Mieloszyk, M., Krawczuk, M., Zak, A., Ostachowicz, W. An Adaptive Wing for a Small Aircraft Application with a Configuration of Fiber Bragg Grating Sensors. *Smart Materials and Structures*, **19 (8)**,pp. 1-12, (2010).
[4] Dragran, K., Klimaszewski, P., Kudela, P., Malinowski, P., Wandowski, T. Health Monitoring of the Helicopter Main Rotor Blades with the Structure Integrated Sensors. *Proceedings of the Fifth European Workshop of Structural Health Monitoring*, pp.69-79, (2010).
[5] Dvorak, M., Ruzicka, M., Kulisek, V., Behal, J., Kafka, V. Damage Detection of the Adhesive Layer of Skin Doubler Specimens Using SHM System Based on Fiber Bragg Gratings. *Proceedings of the Fifth European Workshop on Structural Healh Monitoring*, pp. 70-75, (2010).
[6] Güemes, J.A., Frövel, M., Menendez, J.M., Rodriguez-Lence, F., Menendez Martin, J. Embedded Fiber Bragg Grating as Local Damage Sensors for Composite Materials. *Proceedings of the 8th annual International Symposium on Smart Structures and Materials*, SPIE-4694, San Diego, CA, pp. 118-128, (2002).
[7] Lee, J.R., Ryu, C.Y., Koo, B.Y., Kang, S.G., Hong, C.S., Kim, C.G. In-flight Health Monitoring of a Subscale Wing Using a Fiber Bragg Grating Sensor System. *Smart Materials and Structures*. **12**, pp. 147-155, (2003).
[8] Chambers, A.R., Heinje, N.O. Damage Characterisation in CFRP using Acoustic Emission, X-ray Tomography and FBG Sensors. In *ICCM 17*. Edinburgh, (2009).
[9] Betz, D.C., Staudigel, L., Trutzel. M.N., Kehlenbach, M. Structural Monitoring Using Fiber- Optic Bragg Grating Sensors. In *Structural Health Monitoring: An International Journal*. **2(2)**, pp.145-152, (2003).
[10] Farrar, C.R., Todd, M.D. Introduction to Structural Health Monitoring and Feature Extraction. In *Engineering Institute Workshop*. LA-UR-07-3231, (2006).
[11] Staszewski, W.J., Worden, K. Signal Processing for Damage Detection. In *Health Monitoring of Aerospace Structures: Smart Sensor Technologies and Signal Processing*. John Wiley & Sons Inc., West Sussex, United Kingdom, (2004).
[12] Staszewski, W.J. Advanced Data Pre-processing for Damage Identification based on Pattern Recognition. In *International Journal of Systems Science*. **31(11)**, pp.1381-1396, (2000).
[13] Fassois, S.D., Sakellariou, J.S. Time series methods for fault detection and identification in vibrating structures. In *Philosophical Transactions of the Royal Society: Mathematical, Physical and Engineering Sciences*. VOL. **A365**, pp.411-448, **(**2007**)**.
[14] Cai T.T., and Silverman B.W. Incorporating information on neighboring coefficients into wavelet estimation. *The Indian Journal of Statistics*, **63(b)**, pp. 127-148, (2001).